Inorg. Chem. **2005**, *44*, 2531–2543

Coordination Modes between Copper(II) and *N*-Acetylneuraminic (Sialic) Acid from a 2D-Simulation Analysis of EPR Spectra. Implications for Copper Mediation of Sialoglycoconjugate Chemistry Relevant to Human Biology

Marina Fainerman-Melnikova,[†] Terézia Szabó-Plánka,[‡] Antal Rockenbauer,[§] and Rachel Codd*[,†]

Centre for Heavy Metals Research, School of Chemistry, University of Sydney, NSW 2006, Australia, Department of Physical Chemistry, University of Szeged, P.O. Box 105, H-6701 Szeged, Hungary, and Chemical Research Center, Institute of Chemistry, Hungarian Academy of Sciences, H-1525 Budapest, Hungary

Received July 5, 2004

The equilibrium distribution of species formed between Cu(II) and *N*-acetylneuraminic (sialic) acid (**I**, LH) at 298 K has been determined using a two-dimensional (2D) simulation analysis of electron paramagnetic resonance (EPR) spectra. In acidic solutions (pH values < 4), the major species present are Cu^{2+}, $[CuL]^+$ [logβ = 1.64(4)], and $[CuL_2]$ [logβ = 2.77(5)]. At intermediate pH values (4.0 < pH < 7.5), $[CuL_2H_{-1}]^-$ [logβ = –2.72(7)] and two isomers of $[CuLH_{-1}]$ [logβ (overall) = –3.37(2)] are present. At alkaline pH values (7.5 < pH < 11), the major species present is $[CuL_2H_{-2}]^{2-}$, modeled as three isomers with unique g_{iso} and A_{iso} values [logβ (overall) = –8.68(3)]. Two further species ($[CuLH_{-3}]^{2-}$ and $[CuL_2H_{-3}]^{3-}$) appear at pH values > 11. It is proposed that $[CuL]^+$ most likely features **I** coordinated via the deprotonated carboxylic acid group (O^1) and the endocyclic oxygen atom (O^R) forming a five-membered chelate ring. Select Cu(II)–**I** species of the form $[CuLH_{-1}]$ may feature **I** acting as a dianionic tridentate chelate, via oxygen atoms derived from O^1, O^R, and one deprotonated hydroxy group (O^7 or O^8) from the glycerol tail. Alternatively, **I** may coordinate Cu(II) in a bidentate fashion as the *tert*-2-hydroxycarboxylato (O^1,O^2) dianion. Spectra predicted for Cu(II)–**I** complexes in which **I** is coordinated in either a O^1,O^R {**I**(1–)} or O^1,O^2 {**I**(2–)} bidentate fashion {e.g., $[CuL]^+$ (O^1,O^R), $[CuL_2]$ (bis-O^1,O^R), $[CuLH_{-1}]$ (isomer: O^1,O^2), $[CuL_2H_{-1}]^-$ (O^1,O^R; O^1,O^2), and $[CuL_2H_{-2}]^{2-}$ (isomer: bis-O^1,O^2)} have "irregular" EPR spectra that are ascribed to the existence of Cu(II)–**I**(monomer) ⇌ Cu(II)–**I**(polymer) equilibria. The formation of polymeric Cu(II)–**I** species will be favored in these complexes because the glycerol-derived hydroxyl groups at the complex periphery (O^7,O^8,O^9) are available for further Cu(II) binding. The presence of polymeric Cu(II)–**I** species is supported by EPR spectral data from solutions of Cu(II) and the homopolymer of **I**, colominic acid ($\mathbf{I}_{poly}$). Conversely, spectra predicted for Cu(II)–**I** complexes where **I** is coordinated in a {**I**(2–)} tridentate {e.g., $[CuLH_{-1}]$ (isomer: O^1,O^R,O^7, or O^8) and $[CuL_2H_{-2}]^{2-}$ (isomer: bis-O^1,O^R,O^7, or O^8)} or tetradentate fashion {**I**(3–)} {e.g., $[CuLH_{-3}]^{2-}$ (O^1,O^R,O,$^8O^9$)} are typical for mononuclear tetragonally elongated Cu(II) octahedra. In this latter series of complexes, the tendency toward the formation of polymeric Cu(II)–**I** analogues is small because the polydentate **I** effectively wraps up the mononuclear Cu(II) center. This work shows that Cu(II) could potentially mediate the chemistry of sialoglycoconjugate-containing proteins in human biology, such as the sialylated amyloid precursor protein of relevance to Alzheimer's disease.

Introduction

Sialic acids represent a class of about thirty carbohydrate derivatives that play important roles in the physiology of mammals and other animals.[1,2] In humans, the most abundant sialic acid is *N*-acetylneuraminic acid [5-acetamido-3,5-dideoxy-D-glycero-D-galacto-2-nonulosonic acid; **I** (shown as the β-anomer)]; this acidic carbohydrate is present as the

* To whom correspondence should be addressed. Tel: +61-2-9351 4233. Fax: +61-2-9351 3329. E-mail: r.codd@chem.usyd.edu.au.
[†] University of Sydney.
[‡] University of Szeged.
[§] Hungarian Academy of Sciences.

(1) Angata, T.; Varki, A. *Chem. Rev.* **2002**, *102*, 439−469.
(2) Schauer, R.; Kelm, S.; Reuter, G.; Roggentin, P.; Shaw, L. In *Biology of the Sialic Acids*; Rosenberg, A., Ed.; Plenum Press: New York, 1995; pp 7−67.

10.1021/ic049126d CCC: $30.25
Published on Web 03/09/2005

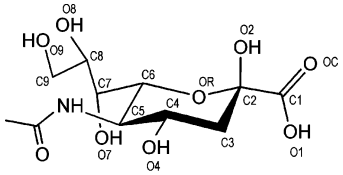

I

terminal residue of glycoprotein and glycolipid (e.g., gangliosides) chains located at cell surfaces and is involved in cell−cell recognition processes and anticoagulation events.[3] The importance of **I** in human biology is widely recognized, in terms of maintaining regular cell function and with respect to its role(s) played in medical conditions, such as influenza[4,5] and alternative disease states.[6] Although **I** has a rich research profile in organic chemistry, only recently has attention turned toward studies of the nature of species formed between transition metal ions and **I**. For example, a study using electron paramagnetic resonance (EPR) spectroscopy detected species formed between oxoCr(V) (d^1) and sialoglycoconjugates derived from human saliva;[7] a complete analysis of the nature of the oxoCr(V)−**I** species formed, in which **I** coordination occurs via the *tert*-2-hydroxycarboxylato "head" group (acidic conditions) or via the glycerol "tail" (alkaline conditions), has subsequently been undertaken using EPR spectroscopic simulation.[8] Since then, oxoCr(V)−**I** speciation has been studied in the presence of Ca(II), which leads to the formation of ternary Ca(II)−oxoCr(V)−**I** complexes that have electronic structures and equilibrium distributions distinct from those of the binary oxoCr(V)−**I** analogues.[9] Lead(II)-induced perturbations to the ^{1}H and ^{13}C NMR spectra of **I** prompted the formulation of a model in which Pb(II)−**I** binding occurs via the carboxylate (O^1)-, ring (O^R)-, and hydroxyl (O^7)-oxygen donor atoms to this soft transition metal;[10] this is similar to the binding motif proposed in early studies of Ca(II)−**I** binding.[11] Additional studies have examined the nature of species formed between **I** and Mn(II), Gd(III), or Eu(III).[12,13] Several metal ions (and one metalloid, Se) have been shown to inhibit the biosynthesis of **I** in vitro via enzyme inhibition mechanisms; Cu(II), for example, inhibited the activity of both UDP-*N*-acetylglucosamine-2′-epimerase and *N*-acetylmannosamine kinase.[14]

Many proteins and lipids in human biology are sialylated.[15−18] The transition metal management proteins, transferrin and ceruloplasmin, for example, have multiantennary sialoglycoconjugates extending into the extracellular milieu.[15,16] Other sialylated proteins of relevance to human biology include the amyloid precursor protein, which yields the β-amyloid peptide associated with Alzheimer's disease,[17] and the polysialylated neural cell adhesion molecule, which is critical to neurogenesis in humans.[18] Because Cu(II) has also been implicated in playing a role in select neurodegenerative diseases involving these proteins and protein products (e.g., β-amyloid peptide),[19−23] it is important to gain insight into the nature of species formed in solution between Cu(II) and **I** as a starting model for more complex systems in human biology.

In the past half decade, a novel technique involving the 2D simulation of EPR spectroscopic data[24] has been used to predict the nature of species (and the logβ values) formed in solution between Cu(II) and bioligands, such as oligoglycines or β-substituted β-amino acids.[25,26] Until now, this 2D-EPR simulation technique had not been applied to Cu(II)−carbohydrate systems; here, we describe our results of the application of the 2D-EPR simulation technique to Cu(II)−**I** solutions at 298 K, including the deconvolution of EPR parameters and formation constants unique to each species and the assignment of the most likely structures of Cu−**I** species based upon these EPR parameters. Results from low temperature (150 K) EPR spectra of glassy solutions of Cu(II)−**I** and Cu(II)−$\mathbf{I}_{poly}$ ($\mathbf{I}_{poly}$ = α-2,8-$\mathbf{I}_n$, where $n \sim 1000$) are also presented. The results from this work implicate a potential role for Cu(II) in sialoglycoconjugate chemistry of relevance to human biology.

Experimental Section

Chemicals. *N*-Acetylneuraminic acid (**I**, sialic acid; Calbiochem, ≥ 98%), colominic acid ($\mathbf{I}_{poly}$, poly-α-2,8-*N*-acetylneuraminic acid, α-2,8-$\mathbf{I}_n$, where $n \sim 1000$, sodium salt from *Escherichia coli*; Sigma), quinic acid (1,3,4,5-tetrahydroxycyclohexanecarboxylic acid, qaH_5; ICN Biomedicals), shikimic acid (3,4,5-trihydroxycyclohexenecarboxylic acid, saH_4; Sigma, 99%), glycerol (gcH_3;

(3) Traving, C.; Schauer, R. *Cell. Mol. Life Sci.* **1998**, *54*, 1330−1349.
(4) Varghese, J. N.; McKimm-Breschkin, J. L.; Caldwell, J. B.; Kortt, A. A.; Colman, P. M. *Proteins* **1992**, *14*, 327−332.
(5) Kiefel, M. J.; von Itzstein, M. *Chem. Rev.* **2002**, *102*, 471−490.
(6) Sillanaukee, P.; Pönniö, M.; Jääskeläinen, I. P. *Eur. J. Clin. Invest.* **1999**, *29*, 413−425.
(7) Codd, R.; Lay, P. A. *J. Am. Chem. Soc.* **2001**, *123*, 11799−11800.
(8) Codd, R.; Lay, P. A. *Chem. Res. Toxicol.* **2003**, *7*, 881−892.
(9) Codd, R. *Chem. Commun.* **2004**, 2653−2655.
(10) Saladini, M.; Menabue, L.; Ferrari, E. *J. Inorg. Biochem.* **2002**, *88*, 61−68.
(11) Jaques, L. W.; Brown, E. B.; Barrett, J. M.; Brey, J. W. S.; Weltner, J. W. *J. Biol. Chem.* **1977**, *252*, 4533−4538.
(12) Daman, M. E.; Dill, K. *Carbohydr. Res.* **1982**, *102*, 47−57.
(13) Sillerud, L. O.; Prestegard, J. H.; Yu, R. K.; Schafer, D. E.; Konigsberg, W. H. *Biochemistry* **1978**, *17*, 2619−2628.
(14) Zeitler, R.; Banzer, J.-P.; Bauer, C.; Reutter, W. *BioMetals* **1992**, *5*, 103−109.
(15) Yamashita, K.; Liang, C. J.; Funakoshi, S.; Kobata, A. *J. Biol. Chem.* **1981**, *256*, 1283−1289.
(16) Zaitseva, I.; Zaitsev, V.; Card, G.; Moshkov, K.; Bax, B.; Ralph, A.; Lindley, P. *JBIC, J. Biol. Inorg. Chem.* **1996**, *1*, 15−23.
(17) McFarlane, I.; Georgopoulou, N.; Coughlan, C. M.; Gillian, A. M.; Breen, K. C. *Neuroscience* **1999**, *90*, 15−25.
(18) Warita, H.; Murakami, T.; Manabe, Y.; Sato, K.; Hayashi, T.; Seki, T.; Abe, K. *Neurosci. Lett.* **2001**, *300*, 75−78.
(19) Brown, D. R.; Kozlowski, H. *J. Chem. Soc., Dalton Trans.* **2004**, 1907−1917.
(20) Barnham, K. J.; McKinstry, W. J.; Multhaup, G.; Galatis, D.; Morton, C. J.; Curtain, C. C.; Williamson, N. A.; White, A. R.; Hinds, M. G.; Norton, R. S.; Beyreuther, K.; Masters, C. L.; Parker, M. W.; Cappai, R. *J. Biol. Chem.* **2003**, *278*, 17401−17407.
(21) Karr, J. W.; Kaupp, L. J.; Szalai, V. A. *J. Am. Chem. Soc.* **2004**, *126*, 13534−13538.
(22) Carroll, M. C.; Girouard, J. B.; Ulloa, J. L.; Subramaniam, J. R.; Wong, P. C.; Valentine, J. S.; Culotta, V. C. *Proc. Natl. Acad. Sci. U.S.A.* **2004**, *101*, 5964−5969.
(23) Bush, A. I.; Masters, C. L.; Tanzi, R. E. *Proc. Natl. Acad. Sci. U.S.A.* **2003**, *100*, 11193−11194.
(24) Rockenbauer, A.; Szabó-Plánka, T.; Árkosi, Z.; Korecz, L. *J. Am. Chem. Soc.* **2001**, *123*, 7646−7654.
(25) Nagy, N. V.; Szabó-Plánka, T.; Rockenbauer, A.; Peintler, G.; Nagypál, I.; Korecz, L. *J. Am. Chem. Soc.* **2003**, *125*, 5227−5233.
(26) Árkosi, Z.; Szabó-Plánka, T.; Rockenbauer, A.; Nagy, N. V.; Lázár, L.; Fülöp, F. *Inorg. Chem.* **2003**, *42*, 4842−4848.

Prolabo, analytical grade), *N*-acetylethanolamine ($NAcH_2$; Lancaster, 95%), $CuSO_4 \cdot 5H_2O$ (Prolabo, analytical grade), and $CuCl_2$ (Reanal, analytical grade) were used as received. All of the solutions were prepared using MilliQ purified H_2O.

EPR Spectroscopy at 298 K in a Static System. Spectra were acquired at 298 K on a Bruker (EMX) EPR spectrometer at the X-band frequency (ca. 9.6 GHz) linked to a Bruker field controller (EMX 032T) and gaussmeter (EMX 035M). Spectra were acquired using the following conditions: modulation frequency, 100 kHz; modulation amplitude, 1.07 G (or 3.07 G); conversion time, 5.12 ms; time constant, 10.24 ms; microwave power, 2 mW; and number of scans, 5. The first series of spectra were acquired from solutions of Cu(II) and **I**, where [Cu(II)] = 10 mM and [**I**] = 10, 20, 40, or 100 mM at pH values ranging from 2.38 to 7.42 in increments of ~1.00 pH units. To mitigate against the precipitation of $Cu(OH)_2$ (as determined visually), the order of the addition of stock solutions of reagents was varied depending upon the pH regime of interest; for solutions where pH < 5.0, an aliquot of an aqueous stock solution of **I** was added to an aliquot of an aqueous $CuSO_4$ stock solution and the volume of the solution made up to just below volume. The pH of the solution [measured using a HANNA micro pH meter (HI 9023) and probe (HI 1083B)] was adjusted to the desired value using aliquots (~2−6 μL) of NaOH (1 or 2 M) or HCl (1 or 2 M) before the solution was made to volume with H_2O. For solutions where pH > 5.0, the solutions were prepared by adding an aliquot of NaOH (1 or 2 M) to an aliquot of the **I** stock solution and H_2O, prior to the addition of the aliquot of the $CuSO_4$ solution. A second series of experiments were conducted in which the [Cu(II)] was increased (1, 5, 10, or 20 mM), where [**I**] = 1, 5, 10, or 20 mM, respectively, at constant pH values (i.e., [Cu(II)]/[**I**] = 1:1 at pH = 3.51 ± 0.24 or 5.53 ± 0.10) or where [**I**] = 2, 10, 20, or 40 mM, respectively (i.e., [Cu(II)]/[**I**] = 1:2 at pH = 3.41 ± 0.14 or pH = 5.54 ± 0.17) or where [**I**] = 4, 20, 40, or 80 mM, respectively (i.e., [Cu(II)]/[**I**] = 1:4 at pH = 3.36 ± 0.10 or pH = 5.39 ± 0.05). Spectra were also acquired ([Cu(II)]/[ligand] = 10:40 mM; pH ~ 3.5−6.5) from solutions of Cu(II) and qaH_5, saH_4, gcH_3, or $NAcH_2$.

EPR Spectroscopy at 298 K in a Circulating System. The EPR spectra were recorded at 298 ± 0.2 K using an upgraded JEOL JES−FE3X or a Bruker Elexsys spectrometer under an argon atmosphere in a circulating system with parameters as previously described.[27] Three titrations were carried out using $CuCl_2$ as a mixture of natural isotopes and 0.2 M KCl as the background electrolyte. In the first titration, the initial total Cu(II) concentration $[Cu(II)]_0$ = 5 mM and the initial total ligand concentration $[\mathbf{I}]_0$ = 8 mM; the pH range was from 2.3 to 6 (at pH values > 6, precipitation was observed). In the second titration, $[Cu(II)]_0$ = 2 mM, $[\mathbf{I}]_0$ = 8 mM, and pH = 2.3−12; in the third titration, $[Cu(II)]_0$ = 2 mM, $[\mathbf{I}]_0$ = 40 mM, and pH = 1.8−12.4. The pH values of the freshly prepared stock solutions were adjusted with HCl, and then NaOH added by a Metrohm 765 Dosimat automatic buret; the pH was measured to an accuracy of 0.01 pH units using a Radiometer PHN 240 pH meter equipped with a Metrohm long life combined pH micro electrode, which was calibrated with IUPAC Standard Buffers (Radiometer).

Evaluation of EPR Spectra Acquired at 298 K in a Circulating System. A series of 36 spectra were evaluated with the 2D-EPR program,[24] modified to take into consideration at most 15 EPR-active species and to fit at most 132 parameters. The spectral analysis was preceded by a correction for the curve of the capillary tube. The EPR spectrum of each species was described by the g_{iso} value, the Cu(II) hyperfine coupling constant (A_{iso}), and the field dimension relaxation parameters (α, β and γ), where the different widths of the Cu(II) lines are given as $\sigma_{M_I} = \alpha + \beta M_I + \gamma M_I^2$ (M_I is the magnetic quantum number of the Cu nucleus). The values of A_{iso} and α, β, and γ refer to the ^{63}Cu isotope and are reported in units of gauss (1 G = 10^{-4} T). The spectra of complexes containing either the ^{63}Cu or ^{65}Cu isotope were calculated and added according to their natural abundance. The equilibrium concentrations of the component species were obtained by solving mass-balance equations. The optimization of the EPR parameters and the formation constants of the mass-balance equations for the EPR-active complexes were based upon the minimization of the overall average square deviation (SSQD), which is the sum of the average square deviations for each spectrum (SQD). The quality of fit for the individual spectra was characterized by a noise-corrected regression parameter (R_j) calculated from the SQD.[24] For the comparison of alternative speciation models, the overall regression coefficient (R) for the whole set of spectra (computed from the SSQD) was used. The program also provides the critical value of the difference in overall regression coefficients (ΔR), which indicates the validity of alternative speciation models. Details of the statistical analyses are provided in previous work.[24] A new statistical parameter, the normalized regression coefficient (NR) has been introduced, given by the expression: $NR = 1 - N_{par}(1 - R)$. The critical regression ΔR indicates whether the difference between two models is significant where the number of adjusted parameters (N_{par}) is the same for each model. Because an increase in N_{par} can result in an improved fit between the experimental and simulated data, the introduction of a new species was considered reasonable when the improvement of regression [i.e., the decrease of $(1 - R)$] was faster than the increase of N_{par} (i.e., the model with the largest value of NR was considered the most likely). The formation constant of the EPR-inactive Cu(II)−**I** complex was determined by minimizing the differences in the analytical and calculated total Cu(II) concentrations, on the basis of the signal intensity of the experimental EPR spectra.

EPR Spectroscopy at 150 K. EPR spectra (X-band; frequency ~9.35 GHz) were acquired at 150 K from water/methanol (75:25) glassy solutions of Cu(II) and **I**, where [Cu(II)]/[**I**] (pH) = 5:8 mM (3.96), 2:8 mM (4.09), 2:8 mM (6.82), 2:8 mM (10.12), 2:40 mM (3.77), 2:40 mM (6.15), or 2:40 mM (10.16) under the following conditions: modulation amplitude, 1.0 G; power, 1.98 mW; and number of scans, 5. Spectra were also acquired of $[Cu(OH_2)_6]^{2+}$ (2 mM) and of Cu(II)−$\mathbf{I}_{poly}$ glassy solutions, where [Cu(II)]/[$\mathbf{I}_{poly}$] = 10:10 mM at pH = 3.80 or 6.64. Spectra were simulated using the program EPR.[28]

Mass Spectrometry. Mass spectra were obtained by the electrospray ionization (ESI) method with samples [$MeOH/H_2O$ (~1:9)] loaded onto the high-performance liquid chromatography pump of a Finnigan LSQ mass spectrometer under the following conditions: mobile phase [$MeOH/H_2O$ (~1:1)]; flow rate, 0.20 mL min^{-1}; temperature at capillary, 200 °C; spray voltage, 5.0 kV; sheath gas pressure, 60 psi; and *m*/*z* range, 150−2000. Six solutions with different [Cu(II)]/[**I**] ratios were analyzed (Supporting Information, Table S1). The pH values of the solutions were measured using the HANNA micro pH meter, detailed above. The assignment of Cu(II)−**I** species was supported with simulation of the mass spectra (Supporting Information, Tables S2a and S2b).

(27) Szabó-Plánka, T.; Rockenbauer, A.; Korecz, L. *Magn. Reson. Chem.* **1999**, *37*, 484−492.

(28) Rockenbauer, A.; Korecz, L. *Appl. Magn. Reson.* **1996**, *10*, 29−43.

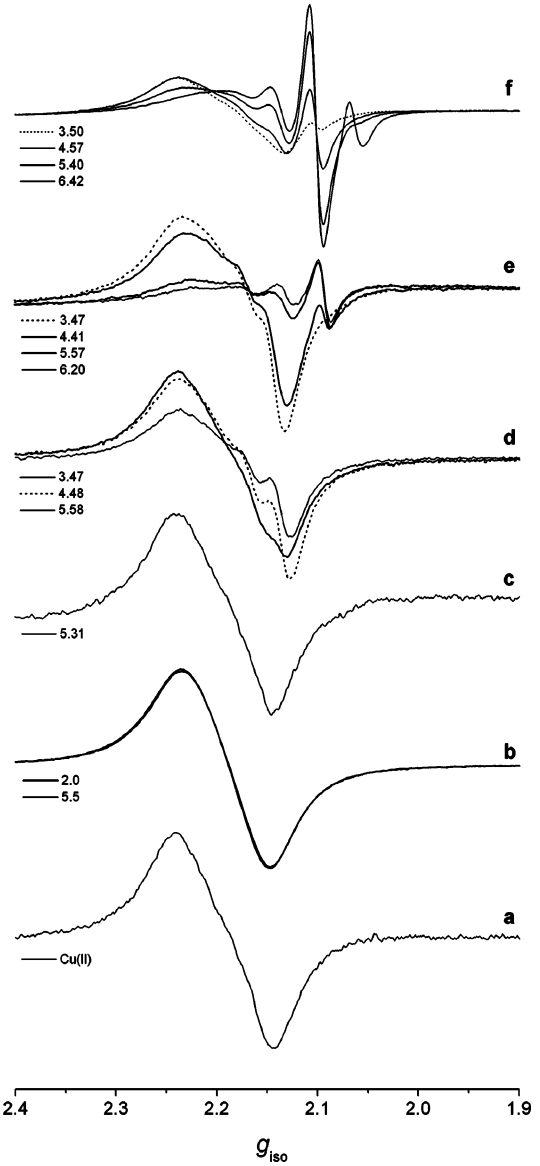

Figure 1. X-band EPR spectra (298 K) from solutions of 10 mM Cu(II) in the absence (a) and presence of 40 mM (b) $NAcH_2$ (pH ~2.0, 5.5), (c) gcH_3 (pH = 5.31), (d) saH_4 (pH = 3.47, 4.58, 5.58), (e) qaH_5 (pH = 3.47, 4.41, 5.57, 6.20), or (f) **I** (pH = 3.50, 4.57, 5.40, 6.42).

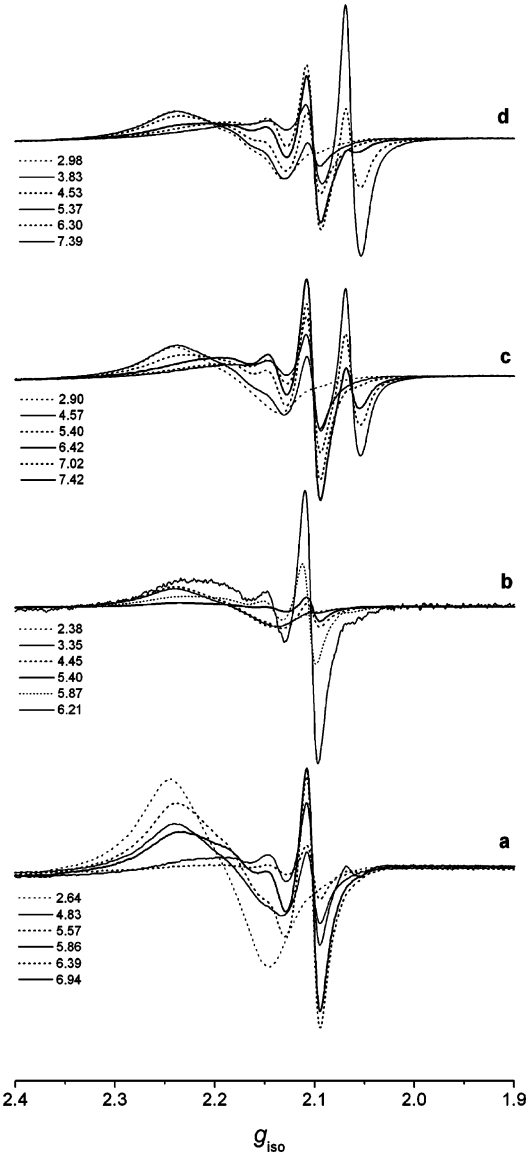

Figure 2. X-band EPR spectra (298 K) from solutions of Cu(II) and **I**, where (a) [Cu(II)]/[**I**] = 10:10 mM (pH values: 2.64, 4.83, 5.57, 5.86, 6.39, 6.94); (b) [Cu(II)]/[**I**] = 10:20 mM (pH values: 2.38, 3.35, 4.45, 5.40, 5.87, 6.21); (c) [Cu(II)]/[**I**] = 10:40 mM (pH values: 2.90, 4.57, 5.40, 6.42, 7.02, 7.42) or (d) [Cu(II)]/[**I**] = 10:100 mM (pH values: 2.98, 3.83, 4.53, 5.37, 6.30, 7.39).

Results

EPR Spectra Acquired at 298 K in a Static System. The EPR spectra acquired from solutions of Cu(II) and **I** at 298 K, where [Cu(II)]/[**I**] = 10:40 mM as a function of pH, show considerable signal complexity (Figure 1f) and are quite distinct from the signal from a solution of free Cu(II), which is broad and featureless ($g_{iso} \sim 2.19$; Figure 1a). Spectra from aqueous solutions of Cu(II) and ligands ([Cu(II)]/[ligand] = 10:40 mM; pH ~ 3.5−6.5) that model isolated regions of **I** ($NAcH_2$, gcH_3, saH_4, or qaH_5) were also acquired (parts b, c, d, and e of Figure 1, respectively).

In the presence of excess $NAcH_2$ or gcH_3, the EPR spectra do not differ significantly from that of free Cu(II), which indicates that Cu(II)−$NAcH_2$ or Cu(II)−gcH_3 complexes are not formed in appreciable concentrations. Cu(II) spectral modulation does occur, however, when Cu(II) is in the presence of an excess of the oxygen-rich, polyfunctional ligands, saH_4, qaH_5, or **I**, with the diminution of the broad signal for free Cu(II) at $g_{iso} = 2.19$ and the appearance of new signals at higher field values. There are similarities in the high field signals from solutions of Cu(II)−qaH_5 or Cu(II)−**I**, which may be attributable to species where coordination involves the *tert*-2-hydroxycarboxylato group (O^1,O^2), because these signals are absent in the Cu(II)−saH_4 system in which this specific binding mode is not possible. In the Cu(II)−**I** system, there is no resolvable ^{14}N A_{iso} superhyperfine coupling to the Cu(II) that would be expected if **I** was coordinating to Cu(II) via the *N*-acetyl group. With increasing [**I**]/[Cu(II)] ratios (from 1:1 to 10:1), the intensity of the signal at $g_{iso} = 2.06$ (which is unique to the Cu(II)−**I** system) increases relative to the signal at $g_{iso} = 2.10$ (Figure 2).

EPR Spectra from Solutions of Increasing [Cu(II)] with Constant [Cu(II)]/[I] and pH Values. Spectra acquired from

Table 1. EPR Parameters[a] and Formation Constants (as logβ)[b] for Cu(II)−**I** Complexes

complex	g_{iso}	A_{iso} (G)	α (G)	β (G)	γ (G)	logβ[b]
Cu^{2+}	2.1946(1)	34.8(2)	53.8(3)	−1.4(1)	0.2(1)	
$[CuL]^{+}$	2.0516(20)	127.0(19)	137.9(8)	55.1(4)	8.4(4)	1.64(4)
$[CuLH_{-1}]$						−3.37(2)[c]
isomer 1	2.1571(1)	50.4(1)	37.9(1)	−16.0(1)	1.4(1)	−3.49(1)
isomer 2	2.1801(7)	84.3(8)	118.7(7)	−167.2(4)	71.3(3)	−3.98(3)
$[Cu_2L_2H_{-4}]^{2-}$						−19.8(2)
$[CuLH_{-3}]^{2-}$	2.1323(2)	71.5(3)	32.1(3)	−18.1(3)	3.3(2)	−23.61(4)
$[CuL_2]$	2.1903(13)	43.4(12)	51.5(4)	−4.7(4)	−2.7(5)	2.77(5)
$[CuL_2H_{-1}]^{-}$	2.0733(15)	28.1(16)	174.9(6)	−10.5(13)	−53.7(8)	−2.72(7)
$[CuL_2H_{-2}]^{2-}$						−8.68(3)[d]
isomer 1	2.1313(1)	63.3(1)	46.0(1)	−32.8(1)	6.2(1)	−9.10(4)
isomer 2	2.1527(2)	97.1(2)	89.8(1)	−80.6(1)	23.1(2)	−9.13(4)
isomer 3	2.1166(1)	55.7(1)	34.5(1)	−19.0(1)	3.1(1)	−9.24(1)
$[CuL_2H_{-3}]^{3-}$	2.1188(7)	75.2(8)	66.5(1)	−42.5(3)	7.6(1)	−21.68(4)

[a] The confidence intervals (3σ) of the last digit at a significance level of 99.7% are given in parentheses. [b] The logβ value LH was taken to be 2.7 (from ref 10). [c] $\log\beta = \log(\beta_{\text{isomer 1}} + \beta_{\text{isomer 2}})$. [d] $\log\beta = \log(\beta_{\text{isomer 1}} + \beta_{\text{isomer 2}} + \beta_{\text{isomer 3}})$.

solutions of Cu(II) and **I** where [Cu(II)] is increased, under conditions of constant [Cu(II)]/[**I**] and pH (Supporting Information, Figure S1), differ within each pH regime studied (pH ∼3.4 and pH ∼5.4), with the signal at the high field increasing in intensity with increasing [Cu(II)]. This suggests that there exists an equilibrium between monomeric and polymeric Cu(II)−**I** species.[29] Further support for the existence of polymeric Cu(II)−**I** species is provided from structurally characterized Cu(II)−qaH_5 complexes, which feature qaH_5 binding to discrete Cu(II) ions via the *tert*-2-hydroxycarboxylato motif and via the ring-bound vicinal diolato moiety.[30,31] Furthermore, EPR spectroscopic data from solutions of Cu(II) and $\mathbf{I}_{poly}$, the homopolymer of **I**, support the notion that polymeric species may be formed in the Cu(II)−**I** system (detailed below).

2D-Simulation Analysis of EPR Spectra Acquired at 298 K in a Circulating System. The Cu(II)−**I** system was further evaluated using EPR spectra acquired in a circulating system, and the data was analyzed using a 2D simulation method that has been used recently to study speciation in alternative Cu(II)−bioligand systems.[25,26] Briefly, the "second dimension" of the method derives from the simultaneous analysis of the full set of spectra collected under different conditions ([metal]/[ligand], pH). The formation constants together with the EPR parameters unique to each species are provided at the completion of the iteration process, and a series of statistical constraints are used to verify the validity of the model.[24]

The minimal Cu(II)−**I** speciation model that fits the data as modeled by the 2D-EPR simulation method comprises a mixture of the following 11 EPR-active species: Cu^{2+} (aqua complex), $[CuL]^{+}$, $[CuLH_{-1}]$ (two isomers), $[CuLH_{-3}]^{2-}$, $[CuL_2]$, $[CuL_2H_{-1}]^{2}$, $[CuL_2H_{-2}]^{2-}$ (three isomers), and $[CuL_2H_{-3}]^{3-}$ (Table 1). In addition, the presence of an EPR-silent species of the form $[Cu_2L_2H_{-4}]^{2-}$ is inferred from the difference between the total [Cu(II)] used in the experiment and the cumulative [Cu(II)] calculated from the EPR simulation analysis. This minimal model results in an excellent spectral fit with the overall regression coefficient $R = 0.998\,952$ and the normalized regression coefficient NR = 0.9319 (Table 2). The omission of any of the above EPR-active species from the model results in a poorer fit between the simulated and experimental spectra (Figure 3) for spectra recorded near the maximum concentration of the specified complex and is quantified by (i) the decrease in the overall regression coefficient significantly exceeding the critical value and (ii) the reduction in the normalized regression coefficient (Table 2). At a moderate excess of **I** to Cu(II) in the alkaline region, the total [Cu(II)] calculated from the spectral intensities for the best model agree well with the total analytical [Cu(II)]; the omission of the EPR-inactive dimer, $[Cu_2L_2H_{-4}]^{2-}$, causes a significant discrepancy between the values of the calculated and analytical [Cu(II)] (Supporting Information, Figure S2).

Table 2. Statistical Parameters for the Best and Reduced Models in the Cu(II)−I System

omitted species	R	$\Delta R/\Delta R_{critical}$[a]	NR[b]
none	0.998 952	0	0.9319
$[CuLH_{-1}]$[c]	0.998 336	88	0.9019
$[CuLH_{-3}]^{2-}$	0.997 838	159	0.8725
$[CuL_2]$	0.998 555	57	0.9148
$[CuL_2H_{-1}]^{-}$	0.998 803	21	0.9294
$[CuL_2H_{-2}]^{2-}$, [c]	0.998 090	123	0.8873
$[CuL_2H_{-2}]^{2-}$, [d]	0.981 826	2447	0.0368
$[CuL_2H_{-3}]^{3-}$	0.998 340	87	0.9021

[a] ΔR is the difference in the overall R values for the best and the reduced models ($\Delta R_{critical} = 0.000\,007$). [b] Normalized regression coefficient (NR), where $NR = 1 - N_{par}(1 - R)$. [c] One of the isomers is neglected. [d] Two of the isomers are neglected.

This deconvolution analysis ultimately yields unique EPR parameters for each of the Cu(II)−**I** species (Table 1; Figure 4) that comprise the parent Cu(II)−**I** solutions together with equilibrium distributions of species under specific concentration ([Cu(II)]/[**I**]) and pH regimes (Figure 5).

Confidence of Parameters from 2D Simulation Analysis. The signature spectra (Figure 4) calculated from the EPR parameters in Table 1 convey some uncertainty in the EPR parameters for select complexes. The Cu hyperfine structure is either partially resolved or unresolved for Cu^{2+}, $[CuL]^{+}$, $[CuLH_{-1}]$ (isomer 2), $[CuL_2]$, $[CuL_2H_{-1}]^{-}$, and $[CuL_2H_{-2}]^{2-}$

(29) Micera, G.; Dessi, A.; Sanna, D. *Inorg. Chem.* **1996**, *35*, 6349−6352.
(30) Barba-Behrens, N.; Salazar-Garcia, F.; Bello-Ramirez, A. M.; Garcia-Baez, E.; Rosales-Hoz, M. J.; Contreras, R.; Flores-Parra, A. *Transition Met. Chem. (London)* **1994**, *19*, 575−581.
(31) Bkouche-Waksman, I. *Acta Crystallogr., Sect. C* **1994**, *C50*, 62−64.

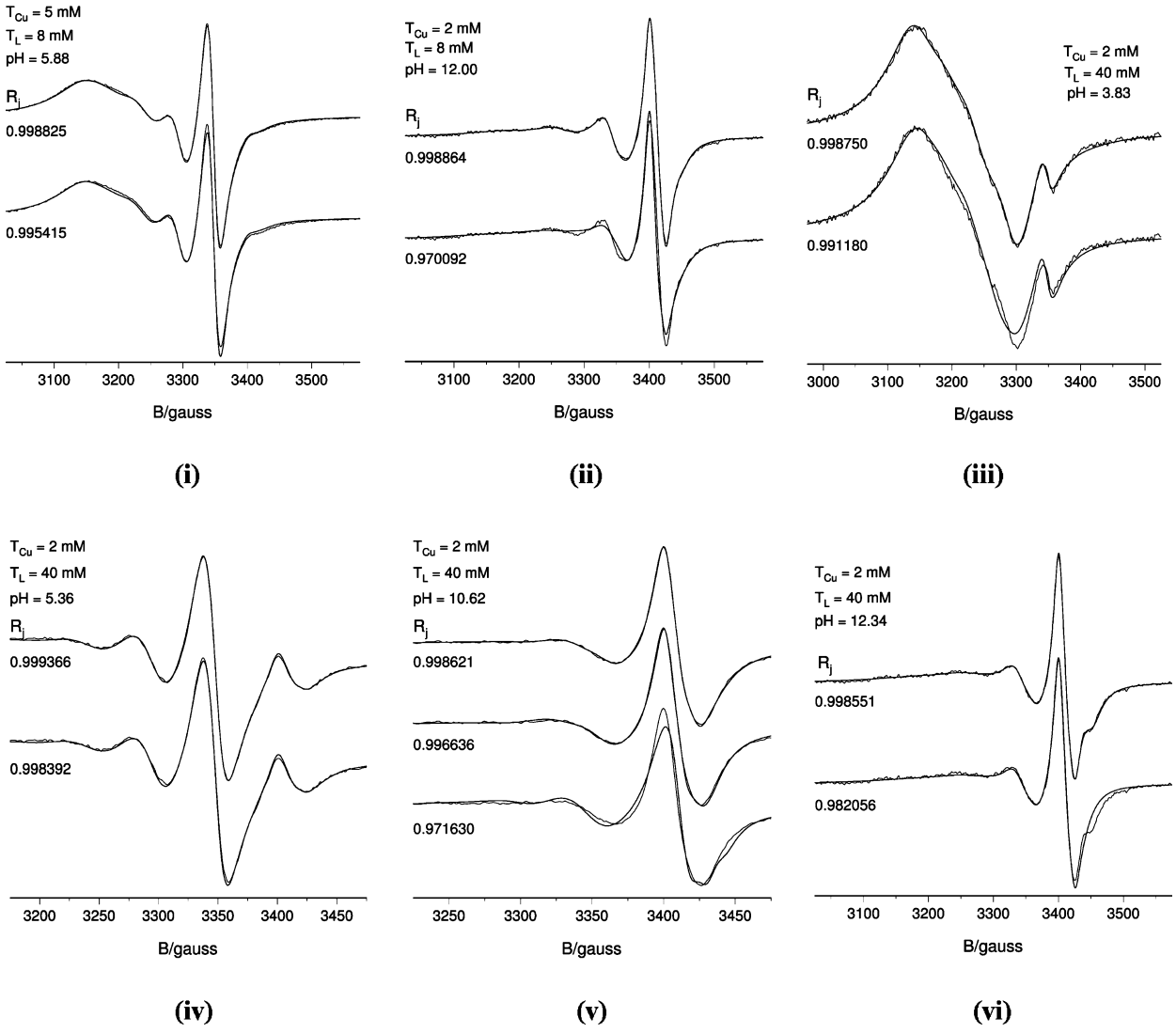

Figure 3. Experimental and calculated EPR spectra in the Cu(II)−**I** system near the maximum concentration of (i) $[CuLH_{-1}]$, (ii) $[CuLH_{-3}]^{2-}$, (iii) $[CuL_2]$, (iv) $[CuL_2H_{-1}]^{-}$, (v) $[CuL_2H_{-2}]^{2-}$, or (vi) $[CuL_2H_{-3}]^{3-}$ for the best model (upper trace) and for the model (middle and lower traces) in which either the species itself (ii, iii, iv, vi) or one (i, v; middle trace) or two (v; lower trace) isomers of the species was omitted.

(isomer 2). Whereas the A_{iso} signal is resolved in the remaining complexes, the low-field lines are broad. It is likely that a significant contribution to this strong magnetic quantum number dependence upon the line width may be caused by the incomplete averaging of the *g* and *A* anisotropy that can occur when the rate of molecular tumbling is slow on the EPR time scale (as might be the case, for example, if polymeric Cu(II)−**I** species were present). The likely origin of the irregular EPR signals for $[CuL]^{+}$, $[CuLH_{-1}]$ (isomer 2), $[CuL_2]$, $[CuL_2H_{-1}]^{2+}$, and $[CuL_2H_{-2}]^{2-}$ (isomer 2) is discussed further below.

Equilibrium Distribution of Cu(II)−I Species. Even at a small excess of **I**, $[CuL]^{+}$ is formed in a relatively high concentration, which indicates the stability of this species (Figure 5). The formation of $[CuL]^{+}$ is also evident under the conditions used in ESI mass spectrometry experiments in both negative (Supporting Information, Table S2a, species D1) and positive (Table S2b, species D, E1, E2) ion modes. Other Cu(II)−**I** species identified under nonequilibrium conditions from mass spectrometry analysis are $[CuLH_{-1}]$ (Table S2a, species D2), $[CuL_2]$ (Table S2a, species H; Table S2b, species L), and $[CuL_2H_{-1}]^{-}$ (Table S2a, species F, J; Table S2b, species M).

Colominic Acid. EPR spectra acquired from solutions of Cu(II) and $\mathbf{I}_{poly}$ at pH values ∼ 3.0 (Supporting Information, Figure S3) showed signals similar (although of lower intensity) to those from Cu(II) and **I**; the signal at $g_{iso} = 2.08$, which appears in the Cu(II)−$\mathbf{I}_{poly}$ system, is not present in the spectrum of free Cu(II). At higher pH values, the intensity of the Cu(II)−$\mathbf{I}_{poly}$ signal diminishes and the line shape changes to one that more closely represents the Cu(II)−**I** spectra at more alkaline pH values. Electronic absorption spectra from solutions of Cu(II) and $\mathbf{I}_{poly}$, where $[Cu(II)]/[(\alpha\text{-}2,8\text{-}\mathbf{I})_n] = 1{:}1 \times 10^{-3}$ (data not shown), show an increase in both the energy and the intensity of the d−d transition with increasing pH values [$\lambda_{max} = 790$ nm; abs = 0.15 (pH = 2.33); $\lambda_{max} = 715$ nm; abs = 0.22 (pH = 6.64)]. Also, an additional charge-transfer band appears in the Cu(II)−$\mathbf{I}_{poly}$ spectra at pH = 6.64 ($\lambda_{max} = 320$ nm). The complexation between Cu(II) and $\mathbf{I}_{poly}$ suggests that the existence

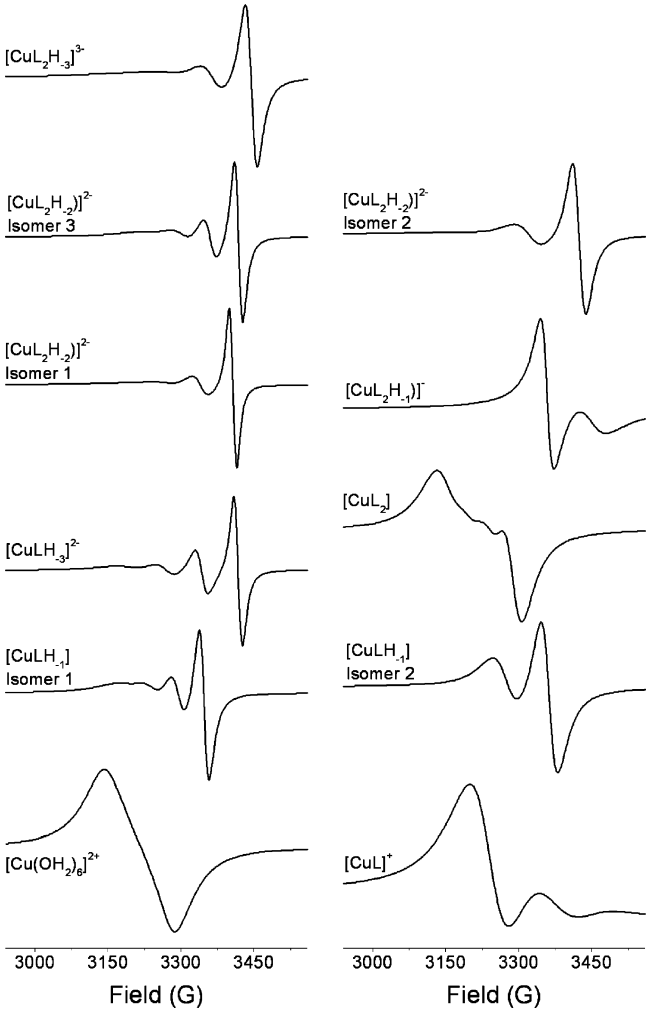

Figure 4. X-Band EPR spectra (9.875 GHz) of individual Cu(II)−**I** species comprising the parent Cu(II)−**I** equilibrium solution at 298 K, showing regular {LHS: $[Cu(OH_2)_6]^{2+}$, $[CuLH_{-1}]$ (isomer 1), $[CuLH_{-3}]^{2-}$, $[CuL_2H_{-2}]^{2-}$ (isomer 1), $[CuL_2H_{-2}]^{2-}$ (isomer 3), and $[CuL_2H_{-3}]^{3-}$} or irregular {RHS: $[CuL]^{+}$, $[CuLH_{-1}]$ (isomer 2), $[CuL_2]$, $[CuL_2H_{-1}]^{2}$, and $[CuL_2H_{-2}]^{2-}$ (isomer 2)} signals, as calculated from the data in Table 1.

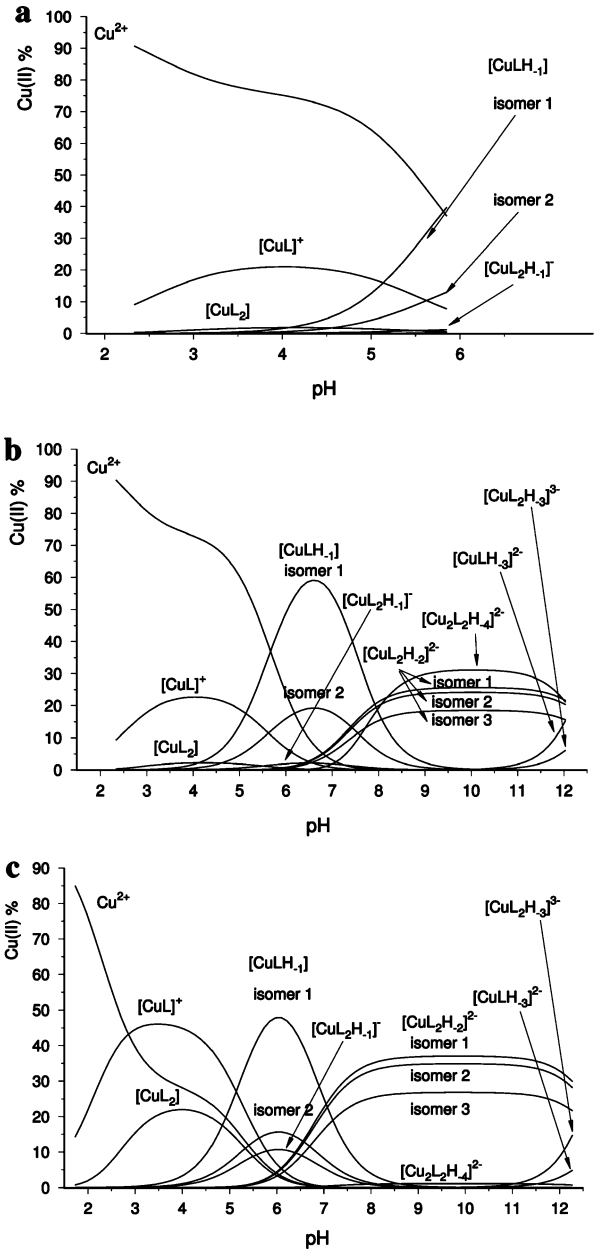

Figure 5. Concentration distribution of Cu(II)−**I** species at 298 K calculated from the EPR spectroscopic formation constants (Table 1) where [Cu(II)]/[**I**] is (a) 5:8 mM, (b) 2:8 mM, or (c) 2:40 mM.

of related polymeric Cu(II)−**I** species is likely to occur under certain conditions.

EPR Spectra Acquired at 150 K. The anisotropic spectrum (water/MeOH at 75:25) from a glassy solution of Cu(II) and **I**, where [Cu(II)]/[**I**] = 2:40 mM and pH = 10.16 (Figure 6d), is similar to the spectrum of $[Cu(acac)_2]$ [acac = acetylacetonoato(1−)][35] in N,N-dimethylformamide (DMF; 130 K), which suggests that the O atoms are the exclusive donors in Cu(II)−**I** complexes under these conditions. As in the spectrum from $[Cu(acac)_2]$, the splitting in the $M_I = -^3/_2A_{||}$ signal in the Cu(II)−**I** system is attributed to the presence of the two Cu isotopes (^{63}Cu, ^{65}Cu) that have different nuclear g values. The EPR parameters of Cu(II)−**I** species that are dominant at acidic pH values (e.g., $[CuLH_{-1}]$) also compare well to those of $[Cu(meac)_2(OH_2)_2]$ (meac = 3,6-dioxaheptanoic acid), which has a Cu(II)−O_6 coordination sphere featuring Cu(II)−O(ether) bonds.[34] There is no discernible resolution of the ^{14}N superhyperfine structure in the $g_\perp$ region of the Cu(II)−**I** EPR signals, which is consistent with the notion that the *N*-acetyl group of **I** is not involved in the Cu(II) coordination sphere, similarly noted from Cu(II)−**I** spectra acquired at 298 K. However, the $g_{||}$ value ($g_{||} = 2.2500$) where [Cu(II)]/[**I**] = 2:40 (pH = 3.77) lies at the low-end extreme of the empirically determined $g_{||}$ value predicted for a Cu(II) complex with four oxygen donors.[36] Taken together with the relatively large $A_{||}$ value under these conditions, this suggests the possibility

(32) Noack, M.; Kokoszka, G. F.; Gordon, G. *J. Chem. Phys.* **1971**, *54*, 1342−1350.
(33) Yordadov, N. D.; Shopov, D. *Dokl. Bulg. Akad. Nauk* **1969**, *22*, 691−694.
(34) Fawcett, J.; Laurie, S. H.; Simpson, C.; Symons, M. C. R.; Taiwo, F. A.; Hawkins, I. *Inorg. Chim. Acta* **2001**, *312*, 245−248.
(35) Howes, B. D.; Kuhlmeyer, C.; Pogni, R.; Basosi, R. *Magn. Reson. Chem.* **1999**, *37*, 538−544.
(36) Peisach, J.; Blumberg, W. E. *Arch. Biochem. Biophys.* **1974**, *165*, 691−708.

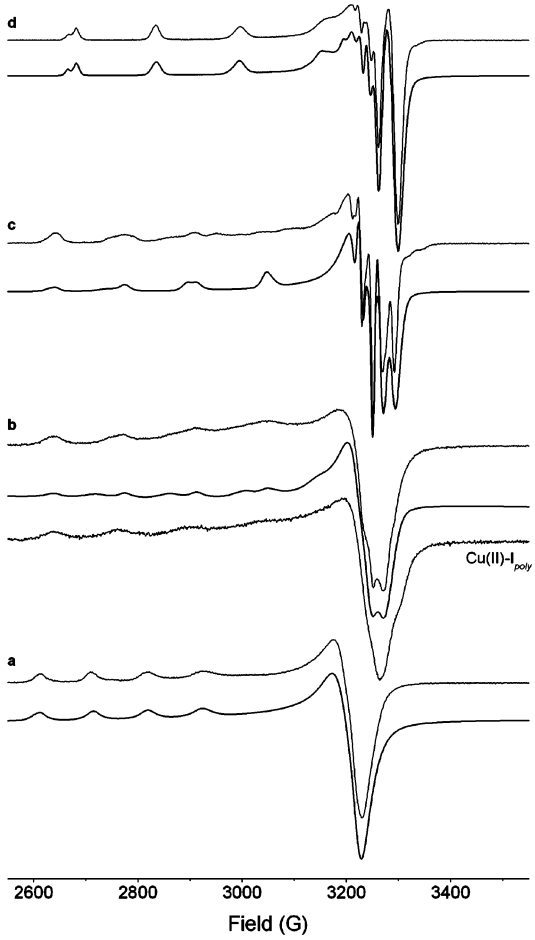

Figure 6. Experimental (black) and simulated (grey) EPR spectra (150 K) from solutions (water/MeOH at 75:25) of (a) Cu(II) (2 mM) or Cu(II)−**I** where [Cu(II)] (mM)/[**I**] (mM) is (b) 2:8 (pH = 4.09), (c) 2:40 (pH = 3.77), or (d) 2:40 (pH = 10.16). The spectrum at the greatest offset in b is from Cu(II) (10 mM) and the homopolymer of **I**, colominic acid ($\mathbf{I}_{poly}$, 10 mM), at pH = 6.64. EPR parameters are given in Table 3.

that Cu(II)−**I** complexes with mixed O- and N-donor atoms may be formed at low temperatures. Further experiments using 3-deoxy-D-glycero-D-galacto-2-nonulosonic acid, in which the *N*-acetyl motif is replaced by a hydroxyl group, will be useful in clarifying this issue. The $A_{||}$ region in the spectra acquired at 150 K (e.g., Figure 6b,c) clearly shows that there is more than one species present in the Cu(II)−**I** system; the presence of multiple species in solutions of Cu(II) and the aminoglycoside, gentamicin, has been similarly proposed on the basis of modulations in the $A_{||}$ region of EPR spectra acquired at 120 K.[37] It is noteworthy that the EPR-silent dinuclear Cu(II)−**I** species ($[Cu_2L_2H_{-4}]^{2-}$) invoked from the 2D-EPR analysis of the Cu(II)−**I** system at 298 K, which is present at the maximum concentration where [Cu(II)]/[**I**] = 2:8 mM (pH 8.5−11.5) (Figure 5), is consistent with decreased [Cu(II)] determined by spin quantitation of the anisotropic Cu(II)−**I** spectra under similar conditions ([Cu(II)]/[**I**] = 2:8 mM, pH = 10.12), even allowing for a considerable error (±15%) that can be associated with this quantitation technique using a single-cavity spectrometer.

Select Cu(II)−**I** spectra acquired at 150 K (Figure 6) were simulated using the program EPR[28] with parameters given in Table 3; the complete set of anisotropic Cu(II)−**I** spectra acquired are provided in Figure S4 (Supporting Information), together with the spin-quantitation data (Figure S5).

The spectrum acquired from a glassy solution of Cu(II) and $\mathbf{I}_{poly}$ ([Cu(II)] = 10 mM; [$\mathbf{I}_{poly}$] = 10 mM, pH = 6.64) at 150 K is very similar to the anisotropic spectrum of Cu(II)−**I**, where [Cu(II)] = 2 mM, [**I**] = 8 mM, and pH = 4.09 (Figure 6; lowest offset trace in b). This is strong support for the proposal that significant concentrations of polymeric Cu(II)−**I** species exist under specific conditions (e.g., where [Cu(II)]/[**I**] = 2:8 mM; pH ∼ 4).

Cross-Checking of the Cu(II)−I Species Proposed Within the 298 and 150 K Temperature Regimes. The 2D-EPR simulation analysis of the Cu(II)−**I** system at 298 K yielded EPR parameters for $[CuL_2H_{-2}]^{2-}$ (isomer 1) of g_{iso} = 2.1313 and A_{iso} = 63.3 G (Table 1). This species is present at the maximum concentration where [Cu(II)]/[**I**] = 2:40 mM at pH values between 8.5 and 11 (Figure 5). The anisotropic spectrum of the Cu(II)−**I** system where [Cu(II)]/[**I**] = 2:40 mM at pH = 10.16 (Figure 6) was simulated (Table 3) as comprising two species; the EPR parameters of the major species (species E; g_{iso} = 2.1326; A_{iso} = 60.90 G) are in excellent agreement with those calculated for $[CuL_2H_{-2}]^{2-}$ (isomer 1). Similarly, the parameters for $[CuLH_{-1}]$ (isomer 1) determined from the 2D-EPR simulation analysis at 298 K (g_{iso} = 2.1571; A_{iso} = 50.4 G) closely mirror the parameters of species C (g_{iso} = 2.1591; A_{iso} = 53.5 G) determined from simulation of the anisotropic spectrum of Cu(II)−**I**, where [Cu(II)]/[**I**] = 2:40 mM and pH = 3.77; under these conditions, $[CuLH_{-1}]$ (isomer 1) is present at appreciable concentrations (Figure 5). The agreement in the EPR parameters calculated for the two dominant species {$[CuL_2H_{-2}]^{2-}$ (isomer 1) and $[CuLH_{-1}]$ (isomer 1)} within the 298 and 150 K temperature regimes provides strong support for the simulation methodologies used within this work.

Discussion

Metal−I Coordination. The consensus of the considerable number of studies of Cu(II)−carbohydrate speciation using potentiometric, polarographic, and calorimetric techniques is that, in the absence of additional functional groups, binding between the carbohydrate diolato groups and Cu(II) is weak.[38,39] This is highlighted in the EPR spectra from solutions of Cu(II) and glycerol [or *cis*- or *trans*-1,2-cyclohexanediol (data not shown)], in which the formation of Cu(II)-diolato (linear- or cyclic-derived) species is not evident. The ligand, **I**, however, is polyfunctional, featuring a *tert*-hydroxycarboxylic acid "head" and a glycerol "tail", in addition to an *N*-acetyl group, an endocyclic oxygen atom, and a 4′-OH group. Therefore, the coordination profile of the Cu(II)−**I** system is likely to be quite distinct from

(37) Lesniak, W.; Harris, W. R.; Kravitz, J. Y.; Schacht, J.; Pecoraro, V. L. *Inorg. Chem.* **2003**, *42*, 1420−1429.

(38) Gyurcsik, B.; Nagy, L. *Coord. Chem. Rev.* **2000**, *203*, 81−149.

(39) Whitfield, D. M.; Stojkovski, S.; Sarkar, B. *Coord. Chem. Rev.* **1993**, *122*, 171−225.

Table 3. EPR Parameters from a Simulation of Cu(II)−I Spectra at 150 K[a]

[Cu(II)]/[**I**][b]	pH	species	$g_\perp$	$g_\parallel$	g_{iso}	$A_\perp$[c]	$A_\parallel$[c]	A_{iso}[c]	concentration[d]
2:0		$[Cu(OH_2)_6]^{2+}$, [e]	2.0814	2.4152	2.1927	11.4	102.3	41.7	1.00
		$[Cu(OH_2)_6]^{2+}$, [f]			2.1946			34.8	
2:8	4.09	A	2.0750	2.3500	2.1667	0	135.0	45.0	0.55
2:8	4.09	B	2.0650	2.2800	2.1367	0	140.0	46.7	0.45
2:40	3.77	C	2.0636	2.3500	2.1591	12.8	135.0	53.5	0.60
		$[CuLH_{-1}]$ (iso1)[f]			2.1571			50.4	
2:40	3.77	D	2.0596	2.2500	2.1231	15.4	150.0	60.27	0.40
2:40	10.16	E	2.0528	2.2921	2.1326	13.3	156.1	60.90	0.884
		$[CuL_2H_{-2}]^{2-}$ (iso1)[f]			2.1313			63.3	
2:40	10.16	F	2.0791	2.3012	2.1531	0	147.7	49.23	0.116
		$[Cu(OH_2)_6]^{2+}$,[g]	2.086	2.379	2.184	17.5	132.4	55.8	1.00
		$[Cu(OH_2)_x(MeOH)_{6-x}]^{2+}$, [h]	2.09	2.34	2.17	ND[i]	99.7	ND	ND
		$[Cu(OH_2)_5(EtOH)]^{2+}$, [g]	2.086	2.425	2.199	ND	113.9	ND	1.00
		$[Cu(meac)_2(OH_2)_2]$[j]	2.067	2.368	2.167	8	137	51	1.00
		$[Cu(acac)_2]$[k]	2.060	2.292	2.137	9.63	153.0	57.42	1.00

[a] Simulated using the program in ref 28. [b] Units of mM. [c] Units of G. [d] Relative concentration from simulation. [e] Values of $A_\parallel$ for $[Cu(OH_2)_6]^{2+}$ are closer to $A_\parallel$ values determined for species of the form $[Cu(OH_2)_x(MeOH)_{6-x}]^{2+}$ (where MeOH is derived from the glassing solvent).[32,33] [f] Species (and EPR parameters) determined from Cu(II)−**I** 2D-simulation analysis at 298 K (refer to Table 1). [g] Reference 32. [h] Reference 33. [i] ND = not determined. [j] Reference 34 (meac = 3,6-dioxaheptanoic acid; 77 K). [k] Reference 35 (DMF; 130 K).

previously examined Cu(II)−carbohydrate systems; in addition, there exists the possibility of the existence of linkage isomers of metal−**I** complexes and polymeric species.

Binding from the *N*-acetyl group of **I** to Cu(II) is improbable because the only functional groups in **I** proximal to the *N*-acetyl group that might serve to "anchor" the ligand to Cu(II) are the 4′-OH group (resulting in a five-membered ring) and the 7′-OH group (resulting in a six-membered ring), both of which are poor Cu(II) donors. While Cu(II)−amide bonds are ubiquitous in Cu(II)-peptide chemistry,[40] these bonds invariably form part of Cu(II)−chelate structures that involve deprotonated carboxylate groups; the carboxylate group in **I** is not correctly configured with respect to the *N*-acetyl group to reasonably invoke *N*-acetyl−Cu(II) binding. Also, structurally characterized complexes formed between Cu(II) and *N*-acetylated amino acids, such as *N*-acetyl-L-aspartate, show that the *N*-acetyl group is not involved in Cu(II) coordination, even when (in the case of *N*-acetyl-D-aspartate) there exists the possibility of forming a stable five- or six-membered chelate ring (with coordination occurring from the α- or β-carboxylate group, respectively).[41] Additional complexes formed between Cu(II) and *N*-acetylated bioligands that have been studied by X-ray crystallography[42] and potentiometry[43] similarly show that the *N*-acetyl group is not involved in the Cu(II)−ligand coordination sphere. This is in agreement with the model proposed for Pb(II)−**I** binding[10] and with an extended X-ray absorption fine structure study of binding between Cu(II) or Zn(II) and the *N*-acetylated polysaccharide, hyaluronate.[44] Superhyperfine coupling (^{14}N) was unresolved in spectra of Cu(II)−**I** species acquired at both 298 and 150 K. Also, metal coordination via the 4′-OH group is unlikely because free **I** occurs predominantly as the β-anomer (α-**I**/β-**I** = 5−8%: 95−92%);[11,45] in the β-conformation (and precluding *N*-acetyl binding), there are no correctly configured neighboring donor groups, with respect to the 4′-OH group, able to form a stable Cu(II)−**I** chelate ring.

Therefore, the functional groups in **I** most likely to bind to Cu(II) are the *tert*-2-hydroxycarboxylato group (O^1,O^2), the glycerol tail (O^7,O^8,O^9), and the endocyclic oxygen atom (O^R). This is in broad agreement with the binding motif suggested for Pb(II)−**I** complexes[10] and for complexes between Cu(II) and **I**-related ligands, such as qaH_5,[30,31] galacturonic acid,[46,47] and tetrahydro-2-furoic acid.[48,49]

Calculated Spectra of Cu(II)−I Species (298 K) from a 2D-EPR Simulation. Of the 11 EPR spectra predicted using 2D-EPR simulation techniques of individual species comprising parent Cu(II)−**I** solutions, 6 show features and parameters (Figure 4, left-hand panel; Table 1) that are "regular" for mononuclear tetragonally elongated Cu(II) octahedra[25,26,50,51] and five have "irregular" spectral features (Figure 4, right-hand panel; Table 1). Specifically, $[CuLH_{-1}]$ (isomer 1), $[CuLH_{-3}]^{2-}$, $[CuL_2H_{-2}]^{2-}$ (isomer 1), $[CuL_2H_{-2}]^{2-}$ (isomer 3), and $[CuL_2H_{-3}]^{3-}$ have "regular" spectra and $[CuL]^+$, $[CuLH_{-1}]$ (isomer 2), $[CuL_2]$, $[CuL_2H_{-1}]^2$, and $[CuL_2H_{-2}]^{2-}$ (isomer 2) have "irregular" spectra. It is suggested that the irregularity of the predicted spectra of the latter set of Cu(II)−**I** complexes arises from the presence of related polymeric species (i.e., in the case of $[CuL]^+$ or $[CuL_2]$, the analogous polymeric species present are $[CuL]_n^+$ or $[CuL_2]_n$, respectively) that would have slow tumbling rates

(40) Farkas, E.; Sóvágó, I. In *Amino Acids, Peptides and Proteins*; Davies, J. S., Ed.; Royal Soceity of Chemistry: Cambridge, U.K., 1998; pp 324−386.
(41) Antolini, L.; Menabue, L.; Saladini, M.; Battaglia, L. P.; Corradi, A. B.; Micera, G. *J. Chem. Soc., Dalton Trans.* **1988**, 909−912.
(42) Corradi Bonamartini, A.; Bruni, S.; Cariati, F.; Battaglia, L. P.; Pelosi, G. *Inorg. Chim. Acta* **1993**, *205*, 99−104.
(43) Casolaro, M.; Chelli, M.; Ginanneschi, M.; Laschi, F.; Messori, L.; Muniz-Miranda, M.; Papini, A. M.; Kowalik-Jankowska, T.; Kozlowski, H. *J. Inorg. Biochem.* **2002**, *89*, 181−190.
(44) Nagy, L.; Yamashita, S.; Yamaguchi, T.; Sipos, P.; Wakita, H.; Nomura, M. *J. Inorg. Biochem.* **1998**, *72*, 49−55.
(45) Dabrowski, U.; Friebolin, H.; Brossmer, R.; Supp, M. *Tetrahedron Lett.* **1979**, *20*, 4637−4640.
(46) Deiana, S.; Gessa, C.; Manunza, B.; Piu, P.; Seeber, R. *J. Inorg. Biochem.* **1990**, *39*, 25−32.
(47) Aruga, R. *Bull. Chem. Soc. Jpn.* **1981**, *54*, 1233−1235.
(48) Michaud, E.; Pivert, G.; Duc, G.; Petit-Ramel, M.; Thomas-David, G. *Can. J. Chem.* **1982**, *60*, 1063−1066.
(49) Erlenmeyer, H.; Griesser, R.; Prijs, B.; Sigel, H. *Helv. Chim. Acta* **1968**, *51*, 339−348.
(50) Halcrow, M. A. *J. Chem. Soc., Dalton Trans.* **2003**, 4375−4384.
(51) Hathaway, B. J. *Struct. Bonding (Berlin)* **1984**, *57*, 55−118.

on the EPR time scale, allowing insufficient averaging of g and A anisotropies. Support for this monomeric ⇌ polymeric equilibrium is found in the EPR spectra acquired from solutions of increasing [Cu(II)] where the [Cu(II)]/[**I**] ratio and the pH value remain constant (Supporting Information, Figure S1). Also, similarly to the Cu(II)−**I** system, EPR spectra from solutions of Cu(II) and galactaric acid show small modulations in the high field region under specific conditions;[52] Cu(II)−galactaric acid complexes have been shown to be polymeric, as determined by X-ray crystallography.[53] The positive value of the relaxation parameter β for $[CuL]^+$ and the negative values of the relaxation parameter γ for $[CuL_2]$ and $[CuL_2H_{-1}]^-$ (Table 1) may be due to dipolar interactions between the paramagnetic centers in the respective polymeric species, $[CuL]_n^+$, $[CuL_2]_n$, and $[CuL_2H_{-1}]_n^-$.

Assignment of the Species [CuL]$^+$. The $[CuL]^+$ species most likely features **I** coordinated to Cu(II) via the deprotonated carboxylic acid group (L^-; reports of the pK_a value of **I** range from ∼2.60[57] to ∼2.70[10]). A five-membered chelate ring may be formed if the endocyclic oxygen atom donates to the Cu(II); this species {$[Cu(O^1,O^R$-**I**$(1-))(OH_2)_4]^+$; Chart 1, **IIa**} would be expected to be more stable than a monodentate or four-membered chelate Cu(II)−carboxylate species (**IIb**). The proposed endocyclic oxygen binding mode in **IIa** is supported by the magnitude of the ratio of logβ ($[CuL]^+$) to pK_a (LH) (Table 4), which is a measure of the relative affinity of L^- toward either a Cu(II) ion (i.e., $L^- + Cu^{2+} \rightleftharpoons [CuL]^+$; forward reaction described by logβ) or a proton [i.e., $L^- + H^+ \rightleftharpoons LH$; forward reaction described by $\log(1/K_a) = pK_a$]. Endocyclic-oxygen containing ligands related to **I**, such as D-galacturonic acid (D-galH) and tetrahydro-2-furoic acid (thfH) have logβ/pK_a values comparable to those of the Cu(II)−**I** system. These values are approximately twice the value for the Cu(II)−acetate system where the ligand acts as a monodentate carboxylate. The binding of **I** to Cu(II) in $[CuL]^+$ via the *tert*-2-hydroxycarboxylato group in which the 2′-OH group remains protonated (Chart 1; **IIc**) is considered unlikely, on the basis of structurally characterized Cu(II)−qaH_5 complexes in which qaH_5 coordinates Cu(II) as the *tert*-2-hydroxycarboxylato-(2−) dianion.[30,31] The irregular line shape of the calculated EPR spectrum of $[CuL]^+$ is most likely due to the formation of polymeric **IIa** units, in which **I** coordinates to one Cu(II) ion via the carboxylate and ring oxygen atoms ("head") and to a second Cu(II) ion via the glycerol tail (Chart 1; $[\mathbf{IIa}]_n$). Polymeric Cu(II)−qaH_5 species featuring *tert*-2-hydroxycarboxylato binding to one Cu(II) ion and to the second ion via the (protonated) ring-derived diolato group have been characterized,[30,31] consistent with $[\mathbf{IIa}]_n$. Mass spectrometry analysis of Cu(II)−**I** solutions (Supporting Information, Tables S1, S2a, and S2b) show multiple high m/z signals that selectively simulate as polymeric Cu(II)−**I** species, although it is unclear whether oligomerization occurs during ionization or whether discrete polymeric Cu(II)−**I** species are present in the solutions analyzed.

Chart 1

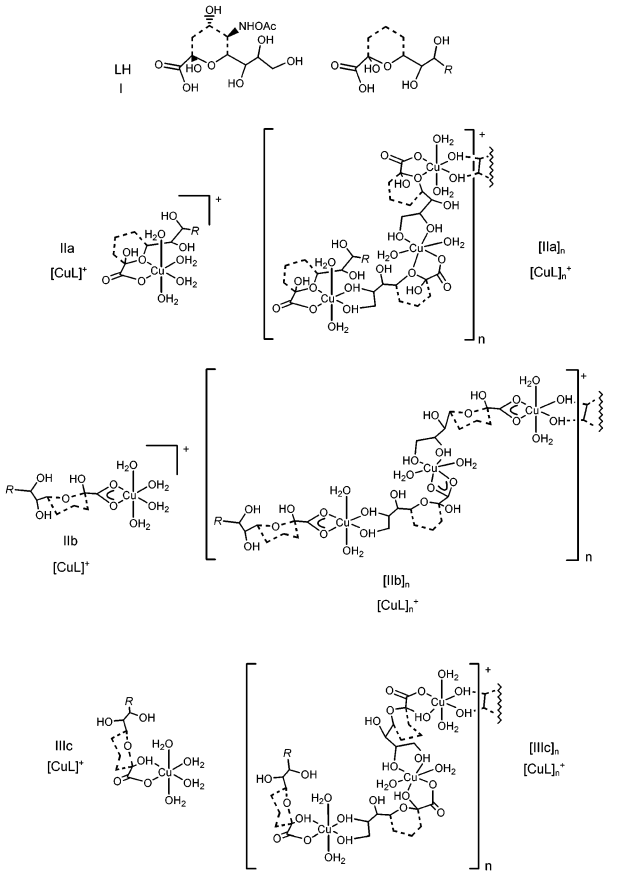

Table 4. Stability Constants (logβ) and logβ/pK_a Values for Complexes Formed between Cu(II) and **I**, D-gal, thfH, or Acetic Acid (acH)

ligand	pK_a	ref	logβ $[CuL]^+$	ref	logβ/pK_a
I	2.7	10	1.64(4)	this work	0.61
D-galH	3.15(1)	54	1.80	54	0.57
D-galH	3.19(1)	55	2.08	55	0.65
thfH	4.96(2)	48	3.47(4)	48	0.70
thfH	4.95(1)	49	3.72	49	0.75
acH	4.56	56	1.76	56	0.39
acH	4.43	47	1.33	47	0.30

Results from potentiometric analysis of Cu(II)−**I** binding[10] have been interpreted as comprising a mixture of Cu^{2+}, $[CuL]^+$, $[CuL_2]$, and $[CuL_2(OH)]^-$; the current work is in agreement in terms of the presence of Cu^{2+}, $[CuL]^+$, and $[CuL_2]$, but it is in disagreement with the relative distributions of these species and with the values of logβ for $[CuL]^+$ [logβ = 3.57(5)] and $[CuL_2]$ [logβ = 6.7(1)], which are considerably greater than the values calculated in the current work. Also, the species $[CuL_2(OH)]^-$ was not observed in the current work; alternate species proposed in the current work are $[CuLH_{-1}]$, $[CuLH_{-3}]^{2-}$, $[CuL_2H_{-1}]^-$, $[CuL_2H_{-2}]^{2-}$, $[CuL_2H_{-3}]^{3-}$, and $[Cu_2L_2H_{-4}]^{2-}$. The interpretation of the

(52) Shestavin, A. I.; Bolotin, S. N.; Volynkin, V. A.; Panyuskhin, V. T. *J. Mol. Liq.* **2003**, *107*, 69−75.
(53) Saladini, M.; Candini, M.; Iacopino, D.; Menabue, L. *Inorg. Chim. Acta* **1999**, *292*, 189−197.
(54) Micera, G.; Dessi, A.; Kozlowski, H.; Radomska, B.; Urbanska, J.; Decock, P.; Dubois, B.; Olivier, I. *Carbohydr. Res.* **1989**, *188*, 25−34.
(55) Escandar, G.; Sala, L. F. *Can. J. Chem.* **1992**, *70*, 2053−2057.
(56) Bunting, J. W.; Kain Men, T. *Can. J. Chem.* **1970**, *48*, 1654−1656.
(57) Hurd, C. D. *J. Chem. Educ.* **1970**, *47*, 481−482.

Chart 2

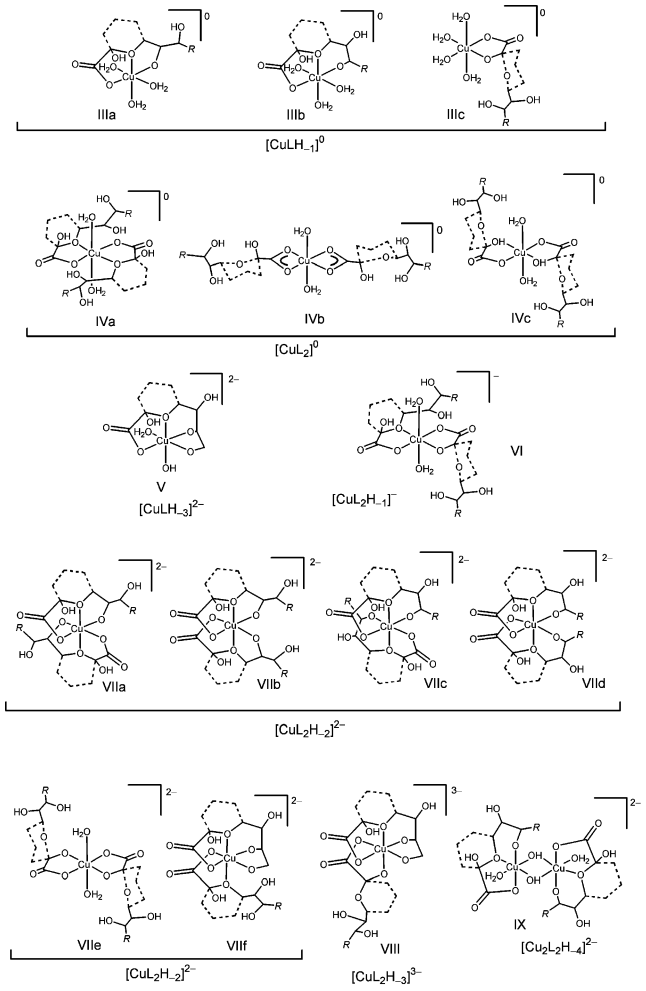

results from the potentiometric study[10] may have been complicated by the precipitation of $Cu(OH)_2$.

Assignment of the Species [CuLH$_{-1}$], [CuL$_2$], [CuLH$_{-3}$]$^{2-}$ and [CuL$_2$H$_{-1}$]$^-$. As the electronic structures of Cu(II)−**I** isomers within a single protonation state become more disparate, EPR spectroscopic parameters unique to each isomer may be more reasonably factored into the model (Figure 3; Table 2). This appears to be the case for the neutral species, [CuLH$_{-1}$]; a significant improvement in the fit between the simulated and experimental data was obtained when this species was modeled as two isomers (Figure 3, panel i). One of the species proposed for [CuLH$_{-1}$] features **I** binding as a tridentate ligand, via O^1, O^R {similar to [Cu(O^1,O^R−**I**(1−))(OH_2)$_4$]$^+$; **IIa**} and one deprotonated hydroxyl group from the glycerol tail, O^7 (**IIIa**) or O^8 (**IIIb**) (Chart 2). The dissociation [CuL]$^+$ ⇌ [CuLH$_{-1}$] + H$^+$ yields a pK_a value = 5.01 (Table 1), which is consistent with the deprotonation of a hydroxyl group [which can be expected to have a lowered pK_a value, induced by the Lewis acidity of Cu(II)].

The tridentate binding of **I** is consistent with the binding mode proposed between **I** and Pb(II)[10] or Ca(II),[11] determined by NMR spectroscopy. Structure **IIIc**, in which **I** is coordinating via the *tert*-2-hydroxycarboxylato(2−) motif {[Cu(O^1,O^2−**I**(2−))(OH_2)$_4$]}, is also consistent with this protonation state. The glycerol tail in **IIIc** is poised for further Cu(II) coordination such as would occur in a polymeric species. As detailed further below, on the basis of the irregular spectrum for [CuLH$_{-1}$] (isomer 2), **IIIc** is the more likely structure of this isomer and structure **IIIa** or **IIIb** is more likely for [CuLH$_{-1}$] (isomer 1). Each of these species (**IIIa**−**IIIc**) has a stronger ligand field compared to that of free Cu(II), which correlates with the decrease in the value of g_{iso} [relative to the g_{iso} value of free Cu(II)] for both isomers of [CuLH$_{-1}$].

The neutral [CuL$_2$] species is formulated here as *trans*-{Cu[O^1,O^R−**I**(1−)]$_2$(OH_2)$_2$} (**IVa**). This complex is formed in low concentration only at a high excess of **I** and has a poorly resolved EPR spectrum. Although two isomers of {Cu[O^1,O^R−**I**(1−)]$_2$(OH_2)$_2$} are possible, in which the carboxylate groups (and correspondingly, the glycerol tails) on each ligand are either in a cis or trans configuration to each other about the *xy* plane of the molecule, the cis isomer is unlikely to be present in significant concentrations, as a result of considerable steric clashes that are present between the glycerol tails. The g_{iso} value for [CuL$_2$] as calculated from the 2D-EPR spectral analysis (g_{iso} = 2.1903) is consistent with the modest shift from the value from free Cu(II) (g_{iso} = 2.1946) that would be expected with the relatively weak donor set in **IVa**. Although structures **IVb** and **IVc** are also consistent with this protonation state, these complexes are predicted to be present in negligible concentrations because of parallel arguments given for the analogous Cu(II)/**I** = 1:1 complexes (i.e., **IIb** and **IIc**). The significant shift in the g_{iso} value for [CuLH$_{-3}$]$^{2-}$ (g_{iso} = 2.1323) from the value for free Cu(II) suggests a strong donor set in the equatorial plane, such as in **V**. It is less likely that [CuLH$_{-3}$]$^{2-}$ represents **IIIa**−**IIIc**, in which two of the aqua ligands are deprotonated, because these complexes would not be expected to have EPR signals with significant Δg_{iso} {where $\Delta g_{iso} = g_{iso}$ (Cu(II)$_{free}$) − g_{iso} (Cu(II)−**I**)} values. In the case of [CuL$_2$H$_{-1}$]$^-$, an (LH$_{-1}$ + L)-type coordination is most probable, as shown in **VI**. The spectrum suggests the existence of a [CuL$_2$H$_{-1}$]$^-$ (monomer) ⇌ [CuL$_2$H$_{-1}$]$_n^-$(polymer) equilibrium, as similarly invoked for [CuL]$^+$. The dissociation [CuL$_2$] ⇌ [CuL$_2$H$_{-1}$] + H$^+$ yields a pK_a value = 5.49 (Table 1), which is consistent with the deprotonation of a hydroxyl group.

Assignment of the Species [CuL$_2$H$_{-2}$]$^{2-}$, [CuL$_2$H$_{-3}$]$^{3-}$, and [Cu$_2$L$_2$H$_{-4}$]$^{2-}$. The Cu(II)−mono-**I**[tridenate(2−)] binding motif proposed for [CuLH$_{-1}$] (isomer 1) (**IIIa**, **IIIb**) translates in a self-consistent manner to the Cu(II)−bis-**I**[tridentate(2−)] protonation state, [CuL$_2$H$_{-2}$]$^{2-}$ (**VIIa**−**VIId**). Here, the proposed species feature two tridentate **I** ligands bound in a meridinal fashion about the Cu(II). There are many possible isomers for the Cu(II)−bis-**I**[tridentate(2−)] formulation; molecular mechanics calculations (in progress) will provide some insight into the most energetically stable species.[58] Several Cu(II) complexes in which two N- or O-containing tridentate ligands coordinate in a meridian fashion have been characterized by X-ray crystallography.[59,60] The 2D-EPR simulation process

(58) New, E. J.; Jolliffe, K. A.; Codd, R. *Work in progress.*

Table 5. Coordination Modes of Cu(II)−**I** Complexes

complex	chelate 1	chelate 2	average	EPR	structure
$[CuLH_{-1}]$ isomer 1	O^1, O^R, O^7, or O^8	N/A	tridentate{**I**(2−)}	regular	**IIIa**, **IIIb**
$[CuLH_{-3}]^{2-}$	O^1, O^R, O^8, and O^9	N/A	tetradentate {**I**(3−)}	regular	**V**
$[CuL_2H_{-2}]^{2-}$ isomer 1	O^1, O^R, O^7, or O^8	O^1, O^R, O^7, or O^8	tridentate {**I**(2−)}	regular	**VIIa**−**VIId**
$[CuL_2H_{-2}]^{2-}$ isomer 3	O^1, O^R, O^8, and O^9	O^1, O^R	tridentate {**I**(2−)}	regular	**VIIf**
$[CuL_2H_{-3}]^{3-}$	O^1, O^R, O^8, and O^9	O^1, O^2	tridentate {**I**(2.5−)}	regular	**VIII**
$[CuL]^+$	O^1, O^R	N/A	bidentate {**I**(1−)}	irregular	**IIa**
$[CuL_2]$	O^1, O^R	O^1, O^R	bidentate {**I**(1−)}	irregular	**IVa**
$[CuLH_{-1}]$ isomer 2	O^1, O^2	N/A	bidentate {**I**(2−)}	irregular	**IIIc**
$[CuL_2H_{-1}]^-$	O^1, O^R	O^1, O^2	bidentate {**I**(1.5−)}	irregular	**VI**
$[CuL_2H_{-2}]^{2-}$ isomer 2	O^1, O^2	O^1, O^2	bidentate {**I**(2−)}	irregular	**VIIe**

reasonably included three isomers of $[CuL_2H_{-2}]^{2-}$ (Table 2; Figure 3, panel v). On the basis of g_{iso} values (Table 1), isomer 2 is most likely to have an (LH_{-1} + LH_{-1})-type coordination, as shown in **VIIa**−**VIIe** (Chart 2). Structure **VIIe** is most consistent with $[CuL_2H_{-2}]^{2-}$ (isomer 2), because the bis-*tert*-hydroxycarboxylato(2−) coordination mode of **I** in **VIIe** leaves the glycerol tails available for further Cu(II) binding that would likely be featured in polymeric species and give rise to an irregular EPR spectrum. This coordination mode is analogous to polymeric Cu(II)−qaH_5 complexes.[30,31] Isomers 1 and 3 of $[CuL_2H_{-2}]^{2-}$ have EPR spectra (Figure 4) that are regular for mononuclear tetragonally elongated Cu(II) octahedra and are assigned to structures **VIIa**−**VIId** or **VIIf** in which concentrations of polymeric analogues are predicted to be small, because **I** will effectively encapsulate the central Cu(II) ion. The relatively large value of Δg_{iso} for isomer 3 (g_{iso} = 2.1166) suggests an (LH_{-2} + L)-type coordination (**VIIf**), featuring **I** coordinated to Cu(II) in a fashion analogous to that of **V**. Isomer 1 of $[CuL_2H_{-2}]^{2-}$, therefore, is assigned to be of the form **VIIa**−**VIId**. The g_{iso} value of $[CuL_2H_{-3}]^{3-}$ suggests this complex has a ligand field strength similar to that of isomer 3 of $[CuL_2H_{-2}]^{2-}$; this condition is met in **VIII**, in which the bidentate **I** ligand coordinates via the *tert*-2-hydroxycarboxylato(2−) motif rather than via the O^1,O^R(1−) mode. The EPR-silent dinuclear species, $[Cu_2L_2H_{-4}]^{2-}$, is formulated as **IX**, in which two Cu(II) ions are antiferromagnetically coupled via two hydroxide bridging ligands.

As the strength of the Cu(II)−**I** donor set increases, the magnitude of Δg_{iso} {where $\Delta g_{iso} = g_{iso}$ [Cu(II)$_{free}$] − g_{iso} [Cu(II)−**I**]} would be expected to increase. This trend is largely consistent for the predicted g_{iso} values and the proposed structures for the Cu(II)−**I** species, although the low g_{iso} value of $[CuL]^+$ is somewhat anomalous (Δg_{iso} = 0.1430), most likely because of complications with the EPR simulation arising from the presence of the Cu(II)−**I**(monomer) ⇌ Cu(II)−**I**(polymer) equilibrium. Because both the carboxylato and endocyclic oxygen atoms are weak donor groups, the g_{iso} value of $[CuL_2]$ (**IVa**; Δg_{iso} = 0.0043) would be predicted to be closest to that of free Cu(II), which is the case here. The species with relatively strong ligand sets, featuring two (**V**, **VIIa**−**VIIf**) or three (**VIII**) alkoxide donor groups, would be predicted to have relatively low g_{iso} values (Δg_{iso} = 0.0419−0.078). The intermediate g_{iso} values (Δg_{iso} = 0.0145−0.0375) of **IIIa**−**IIIc** are consistent in terms of the ligand field strength lying between that of **IVa** (with exclusive O^1, O^R binding) and **VIIa**−**VIIf** (with a higher component of alkoxide character).

Denticity of I in Cu(II)−I Complexes and Correlation with EPR Spectra. Excluding the deconvoluted spectrum of $[Cu(OH_2)_6]^{2+}$ from the following argument (which is in agreement with previous work[24−26]), there is a trend between the "regularity" of each predicted Cu(II)−**I** spectrum and the average denticity of **I** in the complex (Table 5). The tendency for monomeric Cu(II)−**I** complexes to form polymeric analogues might reasonably be related to the denticity of **I** at the Cu(II)−**I** monomeric center; a Cu(II)−**I** complex of low **I** denticity would result in the availability of further Cu(II) donor sites at the complex periphery, compared to a Cu(II)−**I** complex of high **I** denticity in which **I** would more effectively wrap up the mononuclear Cu(II) center.

Where **I** is acting in either a O^1,O^R {**I**(1−)} or O^1,O^2 {**I**(2−)} bidentate fashion, as in $[CuL]^+$ (**IIa**: O^1,O^R), $[CuLH_{-1}]$ (**IIIc**: O^1,O^2), $[CuL_2]$ (**IVa**: bis-O^1,O^R), $[CuL_2H_{-1}]^-$ (**VI**: O^1,O^R; O^1,O^2), and $[CuL_2H_{-2}]^{2-}$ (**VIIe**: bis-O^1,O^2), the predicted EPR spectra are irregular. Complexes in which **I** is acting in either a {**I**(2−)} tridentate {e.g., $[CuLH_{-1}]$ (**IIIa** or **IIIb**: O^1,O^R,O^7, or O^8) and $[CuL_2H_{-2}]^{2-}$ (**VIIa-VIIb**: bis-O^1,O^R,O^7, or O^8)} or {**I**(3−)} tetradentate {$[CuLH_{-3}]^{2-}$ (**V**: O^1,O^R,O^8,O^9)} fashion have spectra that are regular for mononuclear tetragonally elongated Cu(II) octahedra.[25,26,50,51] The predicted EPR spectra for both $[CuL_2H_{-2}]^{2-}$ (isomer 3; **VIIf**) and $[CuL_2H_{-3}]^{3-}$ (**VIII**) are also regular; in these cases (Table 5), the average denticity of **I** is three [i.e., with **I** donating in a tetradentate {**I**(3−)} fashion (O^1, O^R, O^8, and O^9) in one chelate ring (in both **VIIf** and **VIII**) and in a bidentate fashion in the second chelate ring (**VIIf**: O^1, O^R {**I**(1−)}; **VIII**: O^1, O^2 {**I**(2−)})].

Colominic Acid. The glycosidic linkage in $\mathbf{I}_{poly}$ (α-2,8) mitigates against Cu(II)−$\mathbf{I}_{poly}$ binding via the *tert*-2-hydroxycarboxylato motif (or via the 8′-OH group). Therefore, Cu(II)−$\mathbf{I}_{poly}$ binding is most likely to occur via the carboxylic acid group and the endocyclic oxygen atom; at higher pH values, it is also possible that Cu(II) is also coordinated from the deprotonated 7′- or the 9′-OH groups in a fashion similarly invoked for binding between Cu(II) and free **I**. The Cu(II)−$\mathbf{I}_{poly}$ binding is further supported by circular dichroism spectroscopic results, which showed that conformational

(59) Hausmann, J.; Jameson, G. B.; Brooker, S. *Chem. Commun.* **2003**, 2992−2993.
(60) Funahashi, Y.; Kato, C.; Yamauchi, O. *Bull. Chem. Soc. Jpn.* **1999**, *72*, 415−424.

changes to $\mathbf{I}_{poly}$ were induced by Cu(II).[61] The colominic acid system may be a valuable mimic of metal-glycoconjugate biochemistry, because in vivo concentrations of free **I** are small.[6] The similarity between the spectra (150 K) from solutions of Cu(II)−$\mathbf{I}_{poly}$ and Cu(II)−**I** acquired under conditions where $[CuL]^+$ is present in significant concentrations supports the notion that $[CuL]^+$ is in equilibrium with the polymeric species, $[CuL]_n^+$, and corroborates the proposed existence of alternate polymeric Cu(II)−**I** species, the presence of which will most likely occur where **I** is acting in a O^1,O^R {**I**(1−)} or O^1,O^2 {**I**(2−)} bidentate fashion.

Conclusions

The bioinorganic chemistry of **I** is under increasing scrutiny following recent studies that show that **I**, which appears as the terminal residue of cell-bound glycoconjugates, is a viable transition metal ion chelate.[7−10] Because many proteins and lipids of relevance to select human disease states are sialylated, it is pertinent to seek insight into the roles played by the sialyl groups, particularly in diseases, such as Alzheimer's disease, in which metal ions (such as copper) have been implicated.[19−21,23,62] It is possible, for example, that the terminal sialic acid motifs in sialoglyco proteins and lipids play roles above and beyond those of cell−cell recognition and anticoagulation. Intra- and extracellular speciation of transition metal ions is a research area of considerable importance,[63] with implications in better understanding metal homeostasis[64] and metal-mediated diseases.[22]

Here, we have shown, using 2D simulations of EPR spectra, that there are multiple Cu(II)−**I** species formed at equilibrium under conditions that model physiological pH. The particular strength of the EPR simulation techniques used to study Cu(II)−**I** complexes in this work is that within a single protonation state, unique species (i.e., linkage or geometrical isomers) are able to be identified; this is beyond the ability of traditional Cu(II)-bioligand potentiometric studies. The signature binding mode between Cu(II) and **I** most likely involves a chelate formed via the deprotonated carboxylate (O^1) and the endocyclic oxygen atom (O^R); additional coordination from a deprotonated glycerol-derived hydroxyl group sees **I** acting as a tridentate chelate. It is also proposed that select Cu(II)−**I** species form polymeric complexes. Complexes in which **I** acts as a tridentate chelate {e.g., $[CuL_2H_{-2}]^{2-}$ (**VIIa**−**VIId**: bis-O^1,O^R,O^7, or O^8)} have EPR signals typical for mononuclear tetragonally elongated Cu(II) octahedra and are dominant at alkaline pH values. EPR signals of Cu(II)−**I** complexes in which **I** acts in a O^1,O^R {**I**(1−)} or O^1,O^2 {**I**(2−)} bidentate fashion {e.g., $[CuL]^+$ (O^1,O^R), $[CuL_2]$ (bis-O^1,O^R), or $[CuL_2H_{-1}]^-$ (O^1,O^R; O^1,O^2)} are irregular; in these cases, it is proposed that considerable concentrations of the analogous Cu(II)−**I** polymeric species are present that have tumbling rates that do not allow complete averaging of g and A anisotropies. EPR spectra from polymeric Cu(II)−$\mathbf{I}_{poly}$ glassy solutions are very similar to spectra from Cu(II)−**I** glassy solutions acquired under conditions where $[CuL]^+$ is present in significant concentrations, which supports the notion that $[CuL]^+$ exists in equilibrium with the polymeric analogue ($[CuL]_n^+$). The effect of metals such as copper in diseases such as Alzheimer's disease should be examined both in the context of the interaction of the metal at the protein or peptide active site[20,21,23] and in terms of Cu(II)−sialyl interactions that may occur at the protein periphery. The detailed analysis of Cu(II)−**I** and $\mathbf{I}_{poly}$ speciation described here may have significant implications with respect to metal-sialoglycoconjugate chemistry of relevance to human biology.

Acknowledgment. The Sesqui New Staff Support Scheme (University of Sydney) is acknowledged for supporting this work (R.C.) in addition to the Australian Research Council (ARC) and the Wellcome Trust Equipment Fund for the EPR facility (University of Sydney) and the Hungarian Scientific Research Fund (OTKA T:046953) (A.R.). Dr K. Fisher (University of Sydney) is thanked for assistance in the acquisition of the low-temperature Cu(II)−**I** spectra.

Supporting Information Available: EPR spectra (298 K) from solutions of Cu(II) and **I** (where [Cu(II)] is increased and [Cu(II)]/[**I**] and pH are constant) (Figure S1), analytical and calculated total Cu(II) concentrations at 298 K (Figure S2), EPR spectra (298 K) of solutions of Cu(II) and $\mathbf{I}_{poly}$ (Figure S3), EPR spectra (Figure S4) and spin quantitation (Figure S5) from the Cu(II)−**I** system at 150 K, and Tables of Cu(II)−**I** species assigned from ESI mass spectrometry data (Table S1) in both negative (Table S2a) and positive (Table S2b) ion modes are available. This material is available free of charge via the Internet at http://pubs.acs.org.

IC049126D

(61) Koenig, M. K.; McLean, R. J. C. *BioMetals* **1999**, *12*, 47−52.
(62) Casadesus, G.; Smith, M. A.; Zhu, X.; Aliev, G.; Cash, A. D.; Honda, K.; Petersen, R. B.; Perry, G. *J. Alzheimer's Dis.* **2004**, *6*, 165−169.
(63) Finney, L. A.; O'Halloran, T. V. *Science* **2003**, *300*, 931−936.
(64) Culotta, V. C.; Gitlin, J. D. In *The Metabolic & Molecular Bases of Inherited Disease*; Scriver, C. R., Beaudet, A. L., Sly, W. S., Valle, D., Eds.; McGraw-Hill: New York, 2001; pp 3105−3126.